Vol. 13(1), pp. 52-65, January 2019
DOI: 10.5897/AJEST2018.2586
Article Number: 179801159491
ISSN: 1996-0786
Copyright ©2019
Author(s) retain the copyright of this article
http://www.academicjournals.org/AJEST

African Journal of Environmental Science and Technology

Full Length Research Paper

Understanding nexuses between precipitation changes and climate change and variability in semi-arid lowlands of Mwanga District, Tanzania

Bagambilana Francis Rweyemamu and Rugumamu William Mulokozi*

Department of Geography, College of Humanities, University of Dar es Salaam, Tanzania.

Received 25 September, 2018; Accepted 12 November, 2018

Contextually, precipitation fluctuated due to climate variability and evolved due to emissions of anthropogenic greenhouse gases and land-use changes since the industrial revolution in the 1880s. However, some studies problematize that there is little understanding of nexuses between precipitation changes and climate change and variability in tropical Africa. Therefore, this paper sought to assess such linkages in semi-arid lowlands of Mwanga District, Tanzania. The findings revealed statistically significant decrease of annual rainfall, Kendall's tau r_T (44) = -.230, p = .019 and Kendall's tau r_T (39) = -.223, p = .024, at Same Meteorological station (1970 to 2009 and 2012 and 2015) and Nyumba ya Mungu Meteorological stations (1977 to 2015), respectively; thus confirming occurrence of human-induced climate change in the study area. Also, the findings revealed statistically significant correlations between amounts of rainfall (September – February) and Niño 3.4 index and between amounts of rainfall (October – December) and dipole mode index at both stations, hence confirming that precipitation changes during short rainy seasons (*Vuli*) in the lowlands were significantly influenced by cycles of El Niño-southern oscillation and Indian Ocean dipole. Besides, branched and isoprenoid tetraether (BIT) indices revealed that wettest conditions, due to climate variability. This occurred from 650 to 950 CE (common era), 1550 to 1700 CE, 22 to 25 ka BP (before present, present defined as 1950). Whereas, driest conditions occurred from 1968 to 1974, 1780 to 1820 CE, 1170 to 1300 CE (between ca. 0.8 and 0.6 ka BP), 11.7 to 13.1 (the Younger Dryas), 15 to 18 (Heinrich 1 stadial) and 23.4 (Heinrich 2 stadial) ka BP. Lastly, the paper recommends enhancement of traditional and modern-day environmental knowledge systems with regard to weather forecasting and prediction.

Key words: Branched and isoprenoid tetraether index, climate change, climate variability, El Niño-southern oscillation, Indian Ocean dipole, and short rainy season.

INTRODUCTION

According to the intergovernmental panel on climate change (IPCC) (2013), climate fluctuates (climate variability) and evolves (climate change) across space and over time. On the one hand, the main drivers of

*Corresponding author. E-mail: wrugu@udsm.ac.tz.

Author(s) agree that this article remain permanently open access under the terms of the Creative Commons Attribution License 4.0 International License

climate variability include the Indian Ocean dipole (IOD), El Niño-southern oscillation (ENSO), Pacific decadal oscillation (PDO) and Atlantic multidecadal oscillation (AMO). Initially driven by land-sea temperature gradients, atmospheric teleconnections of coupled atmosphere-ocean modes of climate variability lead to extreme weather and climate events, such as droughts and floods at local, meso, synoptic, and planetary spatial scales (Pokhrel et al., 2012; IPCC, 2013; Cassou et al., 2018; Yeh et al., 2018). Cassou et al. (2018) explained, for instance, that devastating droughts and famines of the 1970s and 1980s in the Sahel were associated with changing modes of AMO and PDO.

On the other hand, the main drivers of human-induced climate change, as explained by the theory of greenhouse effect, are accumulation of anthropogenic greenhouse gases in the atmosphere and land-use changes (UN, 1992). To the contrary, however, some scientists, including those affiliated with the Heartland Institute (Bast, 2010) and a nongovernmental international panel on climate change (NIPCC) are skeptical of human-induced climate change or deny the existence of a consensus on the science of human-induced climate change (Stewart, 2008; Inhofe, 2012; Brown, 2013; Idso et al., 2016).

It should be understood that this study adopted a definition of climate change as developed by the United Nations framework convention on climate change (UNFCCC). Specifically, UNFCCC stressed that climate change:

'*Means a change of climate which is attributed directly or indirectly to human activity that alters the composition of the global atmosphere and which is in addition to natural climate variability observed over comparable time periods*' (UN, 1992:7).

Indeed, IPCC's definition reveals that climate change is either caused by natural internal processes/dynamics or external forces, such as modulations of solar cycles (sunspots), volcanic eruptions, orbital parameters (eccentricity, precession, and obliquity), and anthro-pogenic changes in the composition of the atmosphere and land-use change (IPCC, 2013).

Besides, modeling studies projected that shifts of mean climate would increase the frequency, intensity, duration, spatial extent and timing of some extreme weather and climate events (IPCC, 2012; Ostberg et al., 2018). Higher temperatures would lead to, for instance, increasing rates of evapotranspiration, hence increasing severity of droughts on agricultural systems particularly in semi-arid areas (FAO et al., 2018).

According to IPCC (2013), it is very likely that the global water cycle was affected by anthropogenic influences since the 1960s. Such influences (including increasing atmospheric temperatures) led to increases in atmospheric moisture content, global-scale changes in precipitation patterns over land, and intensification of heavy precipitation over land regions where data were sufficient (medium confidence). Under a representative concentration pathway (RCP)8.5 scenario, mean precipitation will likely decrease in many mid-latitude and subtropical dry regions by the end of the 21st century but will likely increase in many mid-latitude wet regions and in the East African region.

On the contrary, some studies, including those undertaken by human-induced climate change skeptics and deniers, suggested that the frequency and intensity of extreme weather events (droughts, floods, and storms) had either decreased or did not reveal any particular trend during recent decades (Stewart, 2008; Inhofe, 2012; Brown, 2013). A study conducted by Laliberté et al. (2015) explained, that warmer periods including the Medieval Climate Anomaly circa (ca.) 900 - 1200 CE and the 20th/21st centuries were associated with a decrease of extreme weather events and that cool periods including the Little Ice Age ca. 1300 to 1900 CE were associated with an increase of unstable and intense weather. IPCC (2013) and Zheng et al. (2018) also supported such findings.

Besides, Verschuren et al. (2000) explained that there is a need to understand long-term precipitation-climate change and variability nexus in order to enhance, among other things, water-resource and land-use management in semi-arid regions of tropical Africa. Indeed, livelihoods of the majority of people in semi-arid tropical Africa were pegged on rain-fed agricultural systems (encompassing sub-systems of crop, livestock, fishery, and forestry production) that were likely to be exacerbated by the interplay between climate change and variability and non-climate drivers and stressors. It should be noted, however, that an understanding of precipitation-climate change and variability nexus in the region was limited by lack of long-term instrumental time series of precipitation. Also, limited high-resolution and well-dated proxy records, such as ice cores and tree rings particularly in areas experiencing bimodal rainfall regime due to biannual passage of inter-tropical convergence zone (ITCZ) (Verschuren et al. (2009).

Indeed, majority of residents in semi-arid lowlands of Mwanga District, Tanzania, which covered 69.4% of the total area of 264,100 ha frequently, faced climate-related stressors, such as meteorological/agricultural droughts, dry spells, and floods (MDC, 2016). These has led to water shortages, land degradation, frequent crop failures, famines (locally known as *Nzota*), and death of domestic animals (Mvungi, 2008; Mashingo, 2010; IFRC and RCS, 2013). Such attributes suggested that precipitation changes in semi-arid lowlands of Mwanga District either reflected human-induced climate change or natural climate variability or both climate change and variability. Coupled with instrumental time series of rainfall and high resolution and well-dated branched and isoprenoid tetraether (BIT) indices for paleo-precipitation, this study

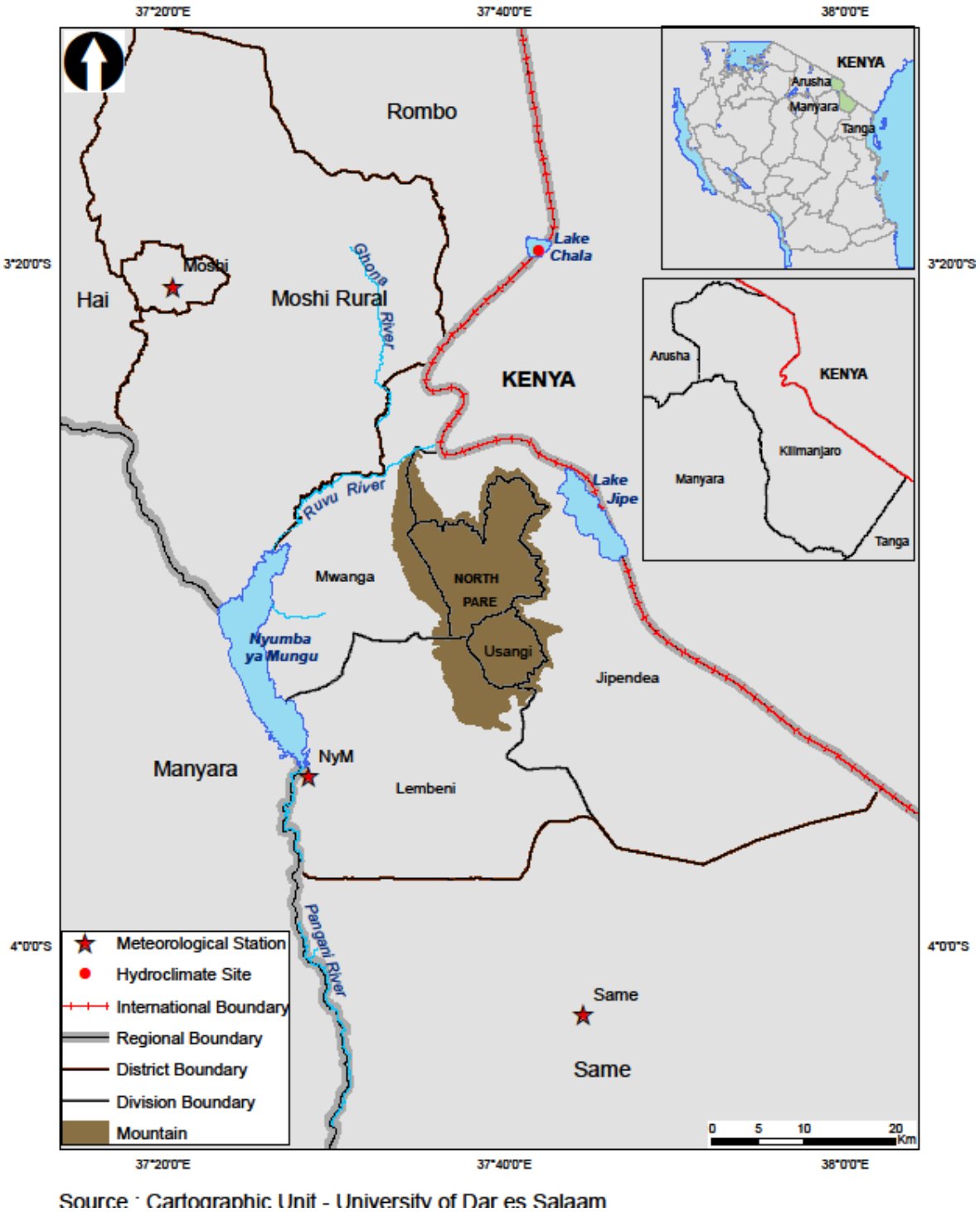

Figure 1. Location of meteorological stations and a hydroclimate site for study area in Mwanga District, Tanzania.

was undertaken in order to understand linkages between precipitation changes in semi-arid lowlands of the district and both climate change and modes of climate variability (El Niño-southern oscillation and Indian Ocean dipole) across different temporal scales.

METHODOLOGY

Study area

Mwanga district (Figure 1) is one of the seven districts of Kilimanjaro Region in northeastern Tanzania and it extends

between latitudes 3°46'S and 3°47' S and between longitudes 37°35'E and 37°50'E (MDC, 2016). Furthermore, the district covers 2,641 km^2 and borders Moshi Rural district and the republic of Kenya in the North, republic of Kenya and Lake Jipe in the East, Same district in the South, and Simanjiro district, NyM Reservoir, and Moshi rural district in the West. Specifically, the district's land areas cover 2,558.6 km^2 while water bodies cover 82.4 km^2. With regard to water bodies, the NyM reservoir covers 56 km^2 and Lake Jipe covers 26.4 km^2 (MDC, 2016).

Furthermore, the regime of rainfall in Mwanga district was bimodal and largely controlled by annual shift in the position of ITCZ and the low-level northeasterly and southeasterly trade winds/monsoons (Moernaut et al., 2010). Specifically, strong and dry winds tended to blow from East to the West (MDC, 2016). Additionally, both ITCZ and trade winds/monsoons were driven by latitudinal differences for radiation, which was received at the Earth's surface (Moernaut et al., 2010). Consequently, long rains (*Mbua ja Mashikaa* in Pare language) were experienced from March to June and short rains (*Mbua ja Vhuri* in Pare language) were experienced from October to January (MDC, 2016).

In addition, the amount of rain varied spatially. Highest amount of rain (800-1350 mm/year) fell in the North Pare Mountains and on its eastern windward slopes to the Indian Ocean and lowest amount of rain (400-600 mm/year) fell in the eastern and western lowlands (URT, 2004; MDC, 2016). Besides, temperatures ranged from an average minimum of 14°C between July and August to a maximum average of 32°C between January and February.

According to IPCC (2013), shifts of climate mean(s) can reliably be detected by analyzing time series data that cover a period of about 50 years. In this regard, attempts were made to source rainfall time series covering longer time periods from meteorological/weather stations within Mwanga District or nearest meteorological/weather stations in Same District (Figure 1). It is worth pointing out that, Pare District was split in 1978 to form Mwanga District in the northern part (MDC, 2016) and Same District in the southern part.

However, rainfall time series for NyM Meteorological Station (station code 9337090) and Same Meteorological Station (station code 9437003) that were sourced from Tanzania meteorological agency (TMA) and Pangani basin water board (PBWB) covered 39 and 44 years, respectively. Indeed, both stations are found in semi-arid lowlands but attempts to harmonize attendant time series would have decreased reliability of analyses for detecting climate change. Otherwise, the same time series were useful for establishing inter-annual climate variability. Besides, rainfall time series covering a period of 62 years (1938 to 1999) at Moshi Meteorological Station (station code 9337004) were sourced from Røhr (2003) as originally sourced from PBWB. Indeed, such time series were used occasionally for comparison with time series for NyM and Same Meteorological Stations. Generally, the computed standardized coefficients of skewness and kurtosis for rainfall time series were positively skewed and < 1.96, hence the coefficients revealed approximate normal distributions.

Also, time series of Niño 3.4 index (sea surface temperature anomalies averaged for areas extending between 5°N and 5°S and between 120° and 170°W in the tropical Pacific Ocean), covering a period of 46 years (1970 to 2015) were accessed through online visits from the national oceanic and atmospheric administration (NOAA). Similarly, time series of dipole mode index (DMI) covering a period of 46 years (1970 to 2015) were accessed through online visits from NOAA. Indeed, DMI time series represented anomalous SST gradient between the western equatorial Indian Ocean (extending between 50°E and 70°E and between 10°S and 10°N) and the southeastern equatorial Indian Ocean (extending between 90° E and 110°E and between 10°S and 0°N).

Moreover, time series for well-resolved BIT index covering periods of the last 2.2 and 25 ka for a hydroclimate of Lake Challa (Figure 1) were accessed online as originally used by Buckles et al. (2016) and Sinninghe Damsté et al. (2012), respectively. It should be noted that Lake Challa is at an altitude of 880 m a.s.l on the lower east slope of Mount Kilimanjaro and along the border between Tanzania and Kenya. Trend analysis (moving averages) was conducted on BIT time series in order to establish patterns of paleo-precipitation with regard to past cycles of climate variability.

Moreover, datasets of rainfall, Niño 3.4 index, DMI, and BIT were entered into spreadsheets (IBM SPSS 20 and or 2007 Excel software) and processed into desired formats. Specifically, datasets of rainfall were cleaned for errors and missing observation values before conducting data analysis. In this regard, the main data cleaning methods were spot-checking, reviewing, and logic checks. It should be noted, however, that a period of two years (January 2010 to December 2011) with missing rainfall time series at Same Meteorological Station, as original time series had not been corrected, was not included in the analysis of meteorological data. Additionally, spatial interpolation could not be conducted with rainfall time series from three meteorological stations (Same, NyM, and Moshi Airport) (Figure 1) as there were no other meteorological/weather stations with relatively longer time series in Mwanga District. According to Tao et al. (2009), the use of deterministic methods (including Inverse Distance Weighted and Spline) and geostatistical methods (including Kriging) of spatial interpolation of climate parameters is worthwhile when there is sufficient density of meteorological/weather stations.

Besides, cleaned datasets of quantitative data were analyzed in IBM SPSS 20 and or 2007 Excel's Analysis ToolPak by computing univariate and bivariate statistics. Specifically, univariate statistics were computed using the following formulas:

1) Mean (*M*)

$$\bar{X} = \frac{\sum_{1}^{n} x_i}{n} \quad (1)$$

Where, $\bar{x}$ = sample mean, n = number of values, x_i = individual value of the sample or measurement (where i goes from 1 to n).

2) Range

$$n = x_{(n)} - x_{(1)} \quad (2)$$

Where, n = range, $x_{(n)}$ = maximum value, $x_{(1)}$ = minimum value.

3) Standard deviation (*SD*)

$$s = \sqrt{\frac{\sum (x_i - \bar{x})^2}{n-1}} \quad (3)$$

Where, s = standard deviation, $\bar{x}$ = sample mean, n = number of values, x_i = individual value of the sample or measurement (where i goes from 1 to n).

4) Anomaly (deviation score)

$$d_i = x - \bar{x} \quad (4)$$

where, d_i = deviation score for the ith observation in a set of observations, x = raw score for observation in a set of observations, $\bar{x}$ = mean of all values in a set of observations.

5) Coefficient of variation

$$cv = \frac{s}{\bar{x}} \quad (5)$$

Where, *cv* = coefficient of variation, *s* = standard deviation, $\bar{x}$ = sample mean.

Furthermore, findings on trends/moving averages were also presented as linear graphs. Additionally, statistical significance of Kendall's tau test was undertaken basing on the following hypotheses:

H_0: There was no trend (data is independent and randomly ordered).
H_1: There was a trend.

In this regard, Kendall's tau r_τ was computed using the following formula:

6) Kendall's tau r_τ

$$\tau = \frac{n_c - n_d}{\frac{1}{2}n(n-1)} \quad (6)$$

Where, τ = Kendall's tau, *n* = sample size, n_c = number of concordant pairs, n_d = number of discordant pairs.

Besides, bivariate analyses encompassed computation of Pearson's correlation coefficient through the following formula:

7) Pearson's correlation coefficient:

$$r = \frac{n\sum xy - \sum x \sum y}{\sqrt{\left[n\sum x^2 - \left(\sum x\right)^2\right]\left[n\sum y^2 - \left(\sum y\right)^2\right]}} \quad (7)$$

Where, *n* = number of pairs of score, $\sum xy$ = sum of the products of paired scores, $\sum x$ = sum of *x* scores, $\sum y$= sum of *y* scores, $\sum x^2$ = sum of squared *x* scores, $\sum y^2$ = sum of squared *y* scores.

It is worth pointing out that alpha level (*α*) was set at 0.05 and the central limit theorem was invoked since the sample size was sufficiently large (usually $N \geq 30$) (Field, 2013). Consequently, the findings based on analysis of quantitative data were largely presented in tables and graphs.

Besides, time series of BIT (branched and isoprenoid tetraether) indices, based on GDGTs (glycerol dialkyl glycerol tetraethers) as proxies for paleo precipitation of Lake Challa area (Figure 1), were sourced through online visits. Indeed, the time series covering a period of the last 2.2 ka were originally used by Buckles et al. (2016) and time series covering a period of the last 25 ka were originally used by Sinninghe Damsté et al. (2012). Additionally, authors through the following formula computed the time series:

8) BIT Index

$$BIT\ index = \frac{[VI] + [VII] + [VIII]}{[V] + [VI] + [VII] + [VIII]} \quad (8)$$

Where, VI = brGDGT VI, VII = brGDGT VII, VIII = brGDGT VIII, V = Crenarchaeol isoGDGTs.

br = branched, iso = isoprenoid, and GDGT = glycerol dialkyl glycerol tetraether

In this regard, times with high BIT values implied existence of drier conditions and times with low BIT values implied existence of wetter conditions (Damsté et al., 2012; Buckles et al., 2016).

RESULTS AND DISCUSSION

This section presents findings and discussions of findings. Specifically, it focuses on instrumental rainfall changes in the study area, nexuses between instrumental rainfall changes in the study area and El niño–southern oscillation and Indian Ocean dipole coupled with BIT indices for paleo-precipitation changes in the study area.

Instrumental rainfall changes in the study area

To begin with, mean annual rainfall at Same Meteorological Station decreased by 235.2 mm from 631.1 mm with a relatively higher SD of 239.4 (1970 to 1979) to 395 mm with a relatively lower *SD* of 73.2 (2012 to 2015) (Table 1). Similarly, mean annual rainfall at NyM Meteorological Station decreased by 250.3 mm from 611.6 mm with a relatively higher *SD* of 170.7 (1977 – 1979) to 361.3 mm with a relatively with lower *SD* of 77.1 (2010 to 2015) (Table 2). Generally, the variability of annual rainfall at NyM Meteorological Station, typified by *SD* of 157.5 for a mean of 342.9 mm and an average coefficient of variation of 0.5 (2077 to 2015), was relatively higher than the variability of rainfall at Same Meteorological Station. This was typified by *SD* of 202.1 for a mean of 540.5 mm and an average coefficient of variation of 0.4 (1970 to 2009 and 2012 to 2015) (Tables 1 and 2).

Also, the findings revealed, during a period of 44 years (1970 to 2009 and 2012 to 2015), increasing negative anomalies of annual rainfall from a reference value of 567.2 mm (an average for a period of 30 years from January 1977 to December 2006) at Same Meteorological Station (Figure 2). Additionally, the fitted linear trend line is statistically significant at alpha level, *α*, of 0.05 (Kendall's tau r_τ (44) = -0.230, *p* = 0.019) (Table 3). Similarly, the findings revealed, during a period of 39 years (1977 - 2015), increasing negative anomalies of annual rainfall from a reference value of 345.5 mm (an average for a period of 30 years from January 1977 to December 2006) at NyM Meteorological Station (Figure 3). In addition, the fitted linear trend line is statistically significant at alpha level, *α*, of 0.05 (Kendall's tau r_τ (39) = -.223, *p* =0.024) (Table 4).

In this regard, positive and negative anomalies of annual rainfall typified annual and inter-annual climate variability. Additionally, increasing negative anomalies of annual rainfall decreased mean annual rainfall, which led

Table 1. Decadal changes in mean annual rainfall at Same Meteorological station, 1970 to 2009 and 2012 to 2015.

Parameter	1970 - 2015	1970 - 1979	1980 - 1989	1990 - 1999	2000 - 2009	2012 - 2015
M	540.5	631.1	559.3	528.5	500.7	395.9
SD	202.1	239.4	122.9	228.4	219.0	73.2
Coefficient of variation	0.4	0.4	0.2	0.4	0.4	0.2
Range	808.7	754.4	391.6	675.5	753.9	169.4
Minimum	265.3	319.6	376.5	299.7	265.3	293.3
Maximum	1074.0	1074.0	768.1	975.2	1019.2	462.7

Source of data: TMA and PBWB.

Table 2. Decadal changes in mean annual rainfall at NyM Meteorological station, 1977 – 2015.

Parameter	1977 - 2015	1977 - 1979	1980 - 1989	1990 - 1999	2000 - 2009	2010 - 2015
M	342.9	611.6	377.6	332.6	226.6	361.3
SD	157.5	170.7	112.5	145.9	142.1	77.1
Coefficient of variation	0.5	0.3	0.3	0.4	0.6	0.2
Range	731.1	338.2	400.8	547.8	487.5	215.4
Minimum	63.2	456.1	198.1	84.3	63.2	272.5
Maximum	794.3	794.3	598.9	632.1	550.7	487.9

Source of data: TMA and PBWB.

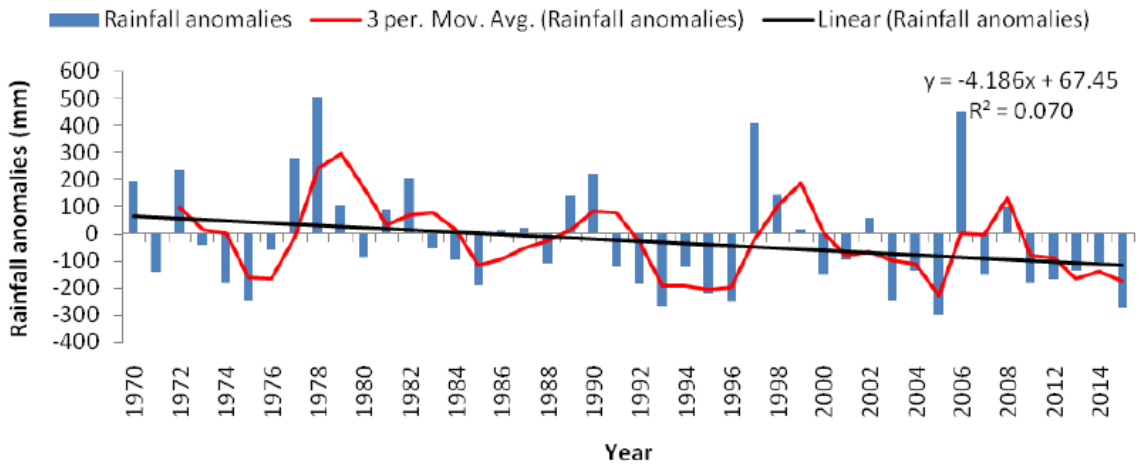

Figure 2. Annual rainfall anomalies for Same Meteorological Station, 1970– 2009 and 2012 – 2015.
Source of data: TMA and PBWB.

Table 3. Mann-Kendall's test for trend of rainfall at Same Met Station, 1970– 2009 and 2012 – 2015.

		Value	Asymp. Std. Error[a]	Approx. T[b]	Approx. Sig.
Ordinal by Ordinal	Kendall's tau-b	-0.230	0.098	-2.349	0.019
	Kendall's tau-c	-0.230	0.098	-2.349	0.019
N of Valid Cases		44			

a. Not assuming the null hypothesis.
b. Using the asymptotic standard error assuming the null hypothesis.

Source of data: TMA and PBWB.

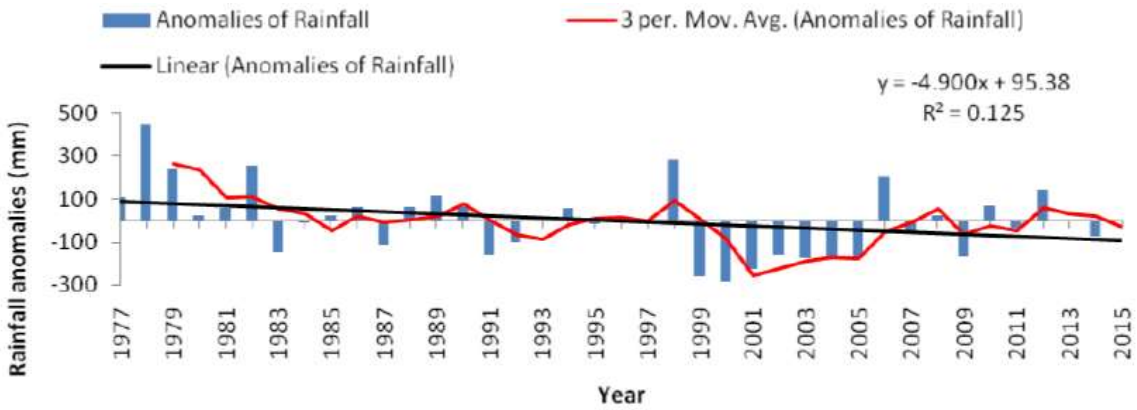

Figure 3. Annual rainfall anomalies for NyM Meteorological Station, 1977– 2015.
Source of data: TMA and PBWB.

Table 4. Mann-Kendall's test for trend of rainfall at NyM Met Station, 1977 – 2015.

Parameter		Value	Asymp. Std. Error[a]	Approx. T[b]	Approx. Sig.
Ordinal by Ordinal	Kendall's tau-b	-0.223	0.098	-2.265	0.024
	Kendall's tau-c	-0.223	0.098	-2.265	0.024
N of Valid Cases		39			
a. Not assuming the null hypothesis.					
b. Using the asymptotic standard error assuming the null hypothesis.					

Source of data: TMA and PBWB.

to climate change. Indeed, rainfall decreased faster at NyM Meteorological Station (slope -4.900 mm y^{-1} and change is explained by 12.5% of the observed variance) than at Same Meteorological Station (slope -4.186 mm y^{-1} and change is explained by 7% of the observed variance) (Figures 2 and 3).

For comparison purposes, the findings did not reveal, during a period of 62 years (1938 – 1999), increasing negative anomalies of annual rainfall from a reference value of 905 mm (an average for a period of 30 years from 1967 to 1996) at Moshi Airport Meteorological Station (Figure 4). Additionally, the fitted linear trend line is non-statistically significant at alpha level, α, of 0.05 (Kendall's tau r_T (62) =.021, p = .810) (Table 5).

It is worth pointing out that climate change is partly caused by land-use/land cover changes (UN, 1992). Furthermore, statistically significant decrease of annual rainfall at both Same and NyM Meteorological stations could partly be explained by land-use/land cover changes. In this regard, a study conducted by Misana et al. (2012) in Kilimanjaro Region (also encompassing semi-arid areas in Mwanga District) revealed, through analyses of satellite images dated 1973, 1984 and 1999/2000, expansion of cultivated areas in the southern and eastern lowlands of Mount Kilimanjaro. This was at the expense of natural vegetation, particularly natural forests in the highlands of Mount Kilimanjaro). Specifically, cultivated areas increased from 54% in 1973, to 62 and 63% in 1984 and 2000, respectively. The main underlying drivers for such land-use/land cover changes were demographic, government policies, socio-economic/cultural factors encompassing land-tenure system, institutional factors, technological change and infrastructure development.

Besides, a study conducted by Huang et al. (2016) revealed that precipitation had decreased by 57 mm in the newly formed semi-arid regions of East Asia during a 61-year period from 1948 to 2008. Additionally, potential evapotranspiration had increased by 132 mm in the same regions and same timescale. A decrease of precipitation and concomitant increase of potential evapotranspiration led to a considerable decrease of aridity index, computed as the ratio of precipitation to potential evaporation, implying an increase of drying trends in the newly formed semi-arid regions of East Asia. The consistency of precipitation patterns with aridity patterns implied precipitation was a key factor influencing aridity index. It is worth pointing out that precipitation had decreased at lesser rate and potential evapotranspiration had increased at lesser rate in the old semi-arid regions of East Asia.

Likewise, a study conducted by Mabhuye et al. (2015)

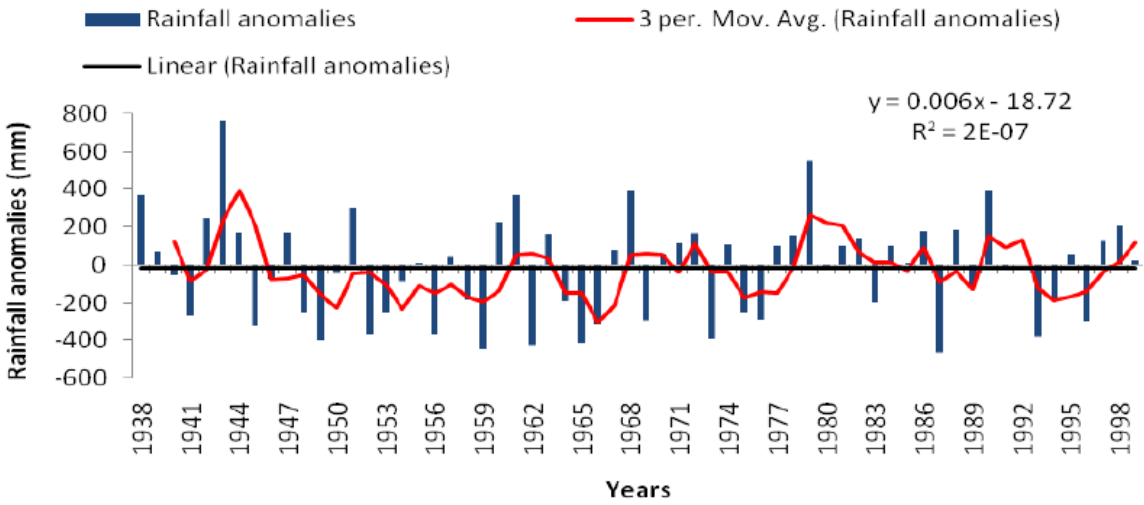

Figure 4. Annual rainfall anomalies for Moshi Airport Meteorological Station, 1938 – 1999.
Source of data: Røhr (2003).

Table 5. Mann-Kendall's test for trend of rainfall at Moshi Airport Met Station, 1938 to 1999.

Parameter		Value	Asymp. Std. Error[a]	Approx. T[b]	Approx. Sig.
Ordinal by Ordinal	Kendall's tau-b	0.021	0.086	0.241	0.810
	Kendall's tau-c	0.021	0.086	0.241	0.810
N of Valid Cases		62			
a. Not assuming the null hypothesis.					
b. Using the asymptotic standard error assuming the null hypothesis.					

Source of data: Røhr (2003).

revealed negative sloping trends for rainfall in most of arid and semi-arid lands of Tanzania during a period from 1975 to 2004. The same study revealed, however, non-significant positive linear trends for annual, MAM (March, April, May), and OND (October, November, December) rainfall for Dodoma during a period from 1960 to 2007.

Besides, a study conducted by IPCC (2013) revealed a high degree of both temporal and spatial variability of precipitation in eastern Africa. Specifically, MAM rainfall had decreased in the region during the previous three decades probably due to rapid warming of the Indian Ocean that led to convection and precipitation over the tropical Indian Ocean and subsidence of drier air over eastern Africa. Additionally, an increasing frequency of dry spells tended to be accompanied with an increasing trend in daily rainfall intensity. Consequently, higher rainfall intensity tended to increase both soil erosion and sediment loads in waterways.

It should be noted, however, that projection of precipitation was much more uncertain than projection of temperature (UNEP, 2012). According to IPCC (2013), an assessment of 12 Coupled Model Intercomparison Project Phase 3 GCMs (general circulation models) over eastern Africa suggested, for instance, a wetter climate with more intense MAM and OND rainy seasons and less severe droughts by the end of the 21st century. During the same time, however, regional climate models indicated that most parts of Kenya, South Sudan, and Uganda would experience drier conditions in August and September due to the weakening of Somali jet and Indian Ocean monsoon. Additionally, it was projected that boreal spring rains would be truncated over eastern Ethiopia, Somalia, Tanzania, and southern Kenya while boreal fall seasons would be lengthened in southern Kenya and Tanzania in the mid-21st century.

Nexuses between rainfall changes in the study area and El niño–southern oscillation and Indian Ocean dipole

An evaluation of the linear relationships between ENSO's Niño 3.4 (five month running mean of extended reconstructed sea surface temperature version 5 (ERSST.v5) anomalies in the Niño 3.4 region from September – February) (Figure 5) and amounts of rainfall

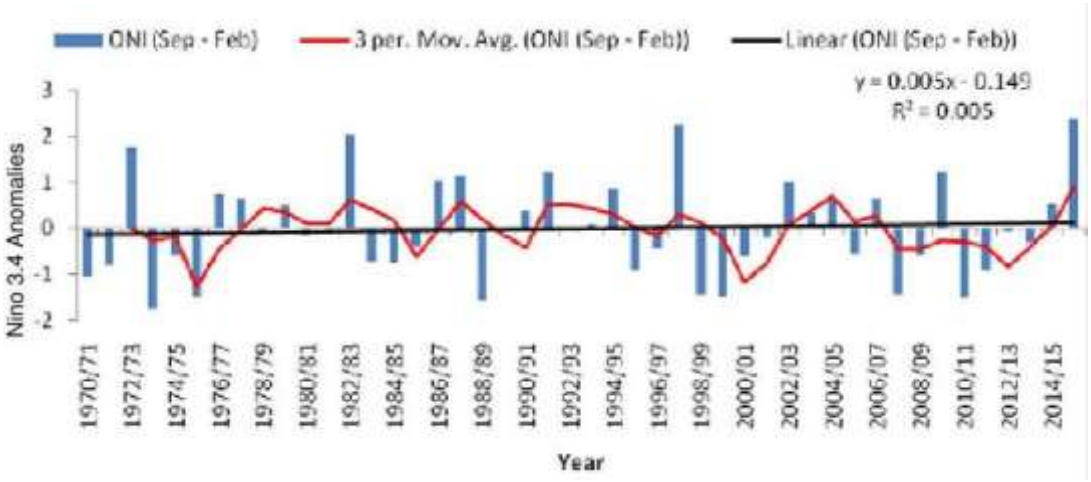

Figure 5. ENSO's Niño 3.4, 1970/71 to 2015/2016.
Source of data: NOAA.

Table 6. Correlation matrix for ENSO's Niño 3.4 and rainfall at Same and NyM meteorological Stations.

		1	2	3
1	ENSO's Niño 3.4 (Sep - Feb)			
2	Sep – Feb rainfall at Same Station	0.54**		
3	Sep – Feb rainfall at NyM station	0.45**	0.85**	

**Correlation is significant at the 0.01 level (2-tailed).

for corresponding periods at Same and NyM Meteorological stations was made through hypothesis testing for statistical significance of Pearson's correlation coefficients.

H_0: ρ = 0 (there was no linear relationship between ENSO's Niño 3.4 and amounts of rainfall during periods from September to February).
H_a: ρ ≠ 0 (there was a linear relationship between ENSO's Niño 3.4 and amounts of rainfall during periods from September to February).

Pearson's correlation coefficient indicated that there was a significant positive linear relationship between ENSO's Niño 3.4 and amounts of rainfall (September – February) at Same Meteorological Station, $r(41) = .54$, $p < .001$ (Table 6), which led to rejection of the null hypothesis. Similarly, there was a significant positive linear relationship between ENSO's Niño 3.4 and amounts of rainfall (September – February) at NyM Meteorological Station, $r(37) = .45$, $p = .004$, which led to rejection of the null hypothesis. Besides, the amounts of rainfall at both stations were highly correlated during a period from September to February, $r(34) = .85$, $p < .001$.

It is worth pointing out that high amounts of rain, 401 mm, 540 mm, and 920 mm, were recorded at Same Meteorological Station from September to February during strong El Niño events of 1972/73, 1982/83, and 1997/98. This was when corresponding Niño 3.4 values were 1.0, 1.3, and 1.4 respectively while low amount of rain, 108.5 mm, was recorded (during the same months) at the same station during a strong La Niña event of 1974/75 when the corresponding Niño 3.4 value was -1.1. Also, high amounts of rain, 421 mm and 598, were recorded (during similar months) at NyM Meteorological Station during strong El Niño events of 1982/83 and 1997/98, when corresponding Niño 3.4 values were 1.3 and 1.4 respectively. However low amounts of rain, 44 and 64 mm, were recorded (during the same months) at the same station during strong La Niña events of 1999/00 and 2000/01 when corresponding Niño 3.4 values were -1.3 and -1.1, respectively.

Similarly, an evaluation of the linear relationships between IOD's DMI (overall anomalies of DMI averaged for periods from October to December) (Figure 6) and the amounts of OND rainfall at Same and NyM Meteorological stations was made through hypothesis testing for statistical significance of a Pearson's correlation coefficient.

H_0: ρ = 0 (there was no linear relationship between IOD's

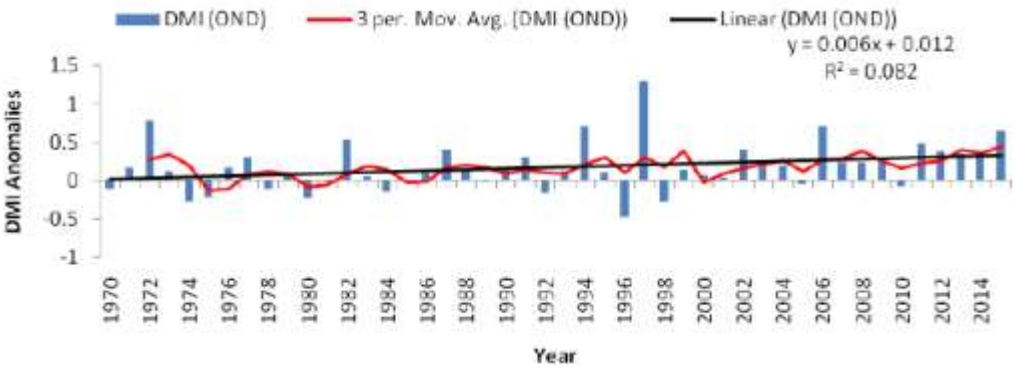

Figure 6. IOD's DMI, 1970 to 2015.
Source of data: NOAA.

Table 7. Correlation matrix for IOD's DMI and rainfall at same and NyM meteorological Stations.

		1	2	3
1	IOD's DMI (OND)			
2	OND rainfall at Same station	0.57**		
3	OND rainfall at NyM station	0.42**	0.71**	

**Correlation is significant at the 0.01 level (2-tailed).

DMI and amounts of OND rainfall).
H_a: ρ ≠ 0 (there was a linear relationship between IOD's DMI and amounts of OND rainfall).

An analysis using Pearson's correlation coefficient indicated that there was a significant positive linear relationship between IOD's DMI and amounts of OND rainfall at Same Meteorological Station, $r(42) = .57$, $p < .001$ (Table 7), which led to rejection of the null hypothesis. Similarly, there was a significant positive linear relationship between IOD's DMI and amounts of OND rainfall at NyM Meteorological Station, $r(37) = .42$, $p = .008$, which led to rejection of the null hypothesis Besides, the amounts of rainfall at both stations were highly correlated during a period from October to December, $r(35) = .71$, $p < .001$.

It is worth pointing out, for example, that high amounts of rain, 400 and 596 mm, were recorded at Same Meteorological Station from October to December during positive IOD phases in 1982 and 1997 when corresponding IOD's DMI values were 0.5 and 0.7, respectively. Furthermore, lower amounts of rain, 29 and 18 mm, were recorded at the same station during negative IOD phases in 1975 and 1996 when corresponding IOD's DMI values were -0.1 and -0.2, respectively. Besides, high amounts of rain, 374 mm and 272, were recorded (during similar months) at NyM Meteorological Station during positive IOD phases in 1982 and 1997 when corresponding DMI values were 0.5 and 0.7 respectively. It should be noted that lower amounts of rain, 0, 15.7, 0, 30, and 38 mm, were recorded (during the same months) at the same station in 1998, 1999, 2000, 2003, and 2005, respectively, when DMI values ranged between 0 and 0.2.

Similarly, Ogwang et al. (2015:7) explained the influence of IOD on East African OND rainfall, hence climate variability in the region.

'Positive IOD (Negative IOD) event results into flood (drought) in the region. The evolution of these phenomena can thus be keenly observed and applied in seasonal forecasting to avert the huge losses associated with extreme weather events. During wet years, the wind circulation is observed to converge in the low levels over the western Indian Ocean and diverge in the upper levels, the opposite is observed in dry years.

Indeed, prolonged periods of drought from 1973 to 1976 for Same Meteorological station (Figure 2) and from 1998 to 2005 for NyM Meteorological station (Figure 3) were largely linked to climate variability. With regard to the former, Kavishe and Mushi (1993) and Limbu (1995) explained that a severe drought of 1973 – 1975 led to crop failure in several parts of Tanzania. Indeed, the drought coupled with Government's implementation of villagization program that displaced farmers and the world's oil crisis led to severe famine, which increased importation of cereals from 12,000 tons in 1972 to 521,000 tons in 1975. Consequently, the drought prompted the Government Tanzania to launch several

campaigns to ensure food security, including *kilimo cha kufa na kupona* (‘Agriculture as a matter of life and death).

With regard to the latter, a study conducted by Kijazi and Reason (2008) established out-of-season peak in January (for years of 1998, 2000, 2001, 2003 and 2004, hence temporary displacement of short (*Vuli*) rainy seasons from OND to NDJ (November, December, January) in the lowlands of northeastern highlands. With respect to the 2004 MAM rainy season, for instance, the onset was on the 14th pentad (period of five days) (6th to 10th March) and the cessation was on the 24th pentad (26th to 30th April), hence a shorter rainy season.

Additionally, total rainfall (169 mm) for the 2004 MAM rainy season was less than half of the normal average of 388 mm. Also, the 2004 MAM rainy season was characterized with unusual dry spells from 16th to 20th March, 6th to 10th April, and 16th to 20th March. According to Kijazi and Reason (2008), the multi-year droughts from 1998 to 2005 were associated with three atmospheric circulation patterns. Firstly, wind circulation patterns diverted atmospheric moisture away from Tanzania. Secondly, there was strong moisture flux divergence in the northeastern highlands. Thirdly, there was strong subsidence, which was linked to the eastward displacement of ascending limb of the Walker-type circulation.

Moreover, both MAM and OND rainy seasons in the study area were largely driven by the yearly double passage of ITCZ between the Equator and Tropic of Capricorn (Owiti et al., 2008; Williams and Hanan, 2011; Schmidt and Spero, 2011). In turn, the migration of ITCZ was largely driven by the intensification and relaxation of migrating Azores and Siberian anticyclones in the northern hemisphere and Mascarene and St. Helena anticyclones in the southern hemisphere.

During January when the overhead Sun was experienced near the southern hemisphere, for instance, the Mascarene and St. Helena anticyclones relatively relaxed in the southern hemisphere while the Azores and Siberian anticyclones intensified in the northern hemisphere. Consequently, the rain-bearing ITCZ was largely confined in the southern hemisphere. Conversely, during July when the overhead Sun was experienced near the northern hemisphere, the Mascarene and St. Helena anticyclones relatively intensified in the southern hemisphere while the Azores and Siberian anticyclones relaxed in the northern hemisphere. Thus, the rain-bearing ITCZ was largely confined in the northern hemisphere.

Paleo-precipitation changes in the study area

To begin with BIT index covering a period of the last 2.2 ka, highest BIT values (> 0.8), implying wettest periods that were accompanied with floods, occurred between 650 and 950 CE, and between 1550 and 1700 CE (Figure 7). To the contrary, lowest BIT values (< 0.5), implying driest periods, occurred between 1170 and 1300 CE, and between 1780 and 1820 CE. In addition, low BIT values occurred between 1870 and 1895 CE and between 1968 and 1974 CE.

In this regard, a study conducted by Scroxton et al., (2017) reported similar wet phases between the 6th and 10th centuries and between the 16th and 18th centuries for: i) Anjohibe speleothem, Madagascar based on $\delta^{18}O$ record, ii) Cave Defore speleothem, Oman based on $\delta^{18}O$ record, iii) Lake Edward, Uganda/Democratic Republic of Congo based on Mg/Ca in Calcite, iv) Lake Naivasha, Kenya, based on Lake level (m), and v) Liang Luar Cave speleothem, Flores, Indonesia based on PC1. Specifically, Verschuren et al. (2000) observed an agreement between (multi-) decadal trends in Lake Challa’s varve thickness record and the 1100-year moisture-balance reconstruction from Lake Naivasha, Central Kenya.

Moreover, such state of affairs was attributed to both zonal Walker Cell dynamics controlled by the Indian Ocean and meridional shifts in the average position of ITCZ that influenced the intensity of northeasterly and southeasterly monsoons/rains. Indeed, monsoon rainfall, controlled by insolation forcing and ENSO dynamics, varied at half-processional (11,500 years) interval (Verschuren et al., 2009; Wolf et al., 2011; Buckles, 2016).

Furthermore, the driest period that occurred between 1110 and 1310 CE was partly associated with a period of high volcanic activity (the Medieval Volcanic Activity) between 1250 and 1500 CE when global temperatures cooled dramatically as explained by the theory of volcanic activity (IPCC, 2013). In addition, a study conducted by Scroxton et al.,(2017) reported similar drier periods between the 11th and 15th centuries and in the 20th century for five hydroclimate stations as mentioned above. Likewise, a study conducted by Verschuren et al. (2000) suggested the existence of drier conditions in Equatorial East Africa during the Mediaeval Warm Period (1000 to 1270 CE) and the relatively wetter conditions during the Little Ice Age (1270 – 1850) that were interrupted by severe drought episodes (1380 to 1420 CE, 1560 to 1620 CE, and 1760 to 1840 CE). Generally, such findings suggested that both zonal and meridional mechanisms controlled tropical precipitation variability during the late Holocene. It should be noted, however, that the relatively drier and windier conditions existed in Lake Malawi, within the African Rift Valley, partly due to the weakening of the Congo Basin Monsoon during the Little Ice Age (Scroxton et al., 2017).

Pertaining to the BIT index covering a period of the last 25 ka, lowest BIT values (< 0.6), implying driest periods, occurred during Heinrich 2 stadial, the late Last Glacial Maximum and early Late-glacial period (including Heinrich 1 stadial) (20.4 - 15.9 ka BP) and during the

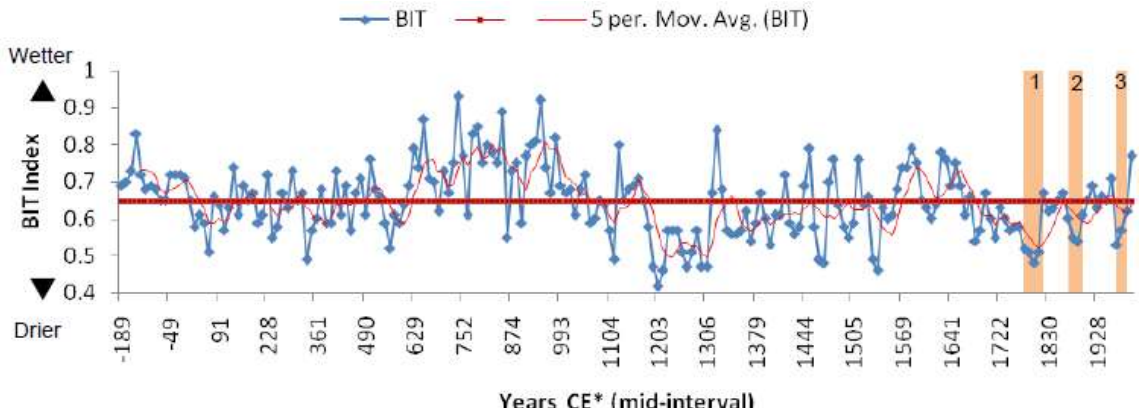

Figure 7. BIT index for Lake Challa area during the last 2.2 ka. Orange-shaded bars approximate periods of documented drought episodes in East Africa: 1 (1780 – 1820 CE), 2 (1870 – 1895 CE), and 3 (1968 – 1974 CE). Source of data: NOAA and Buckles et al. (2016).

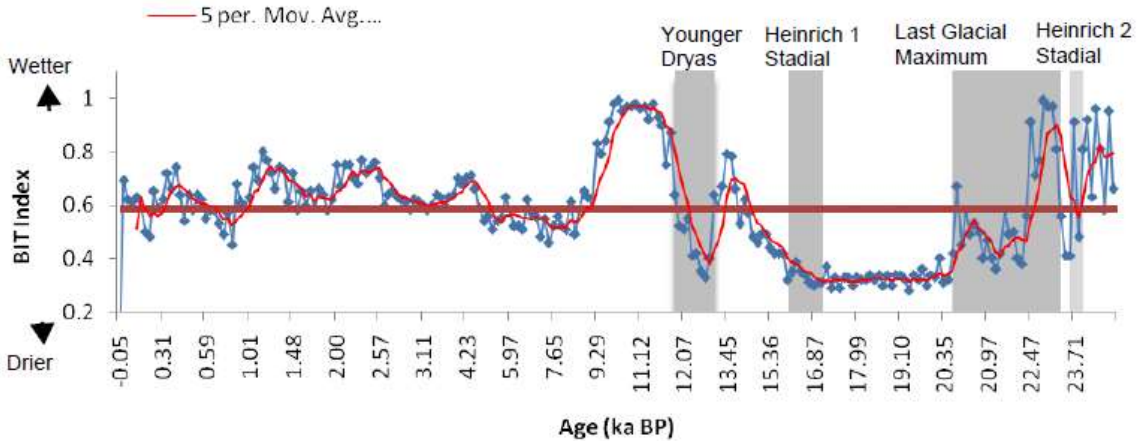

Figure 8. BIT index for Lake Challa area during the last 25 ka.
Source of data: Sinninghe Damsté et al. (2012).

Younger Dryas (13.1 - 11.7 ka BP) (Figure 8). In addition, drier conditions occurred during the mid Holocene (6 ka BP) and late-Holocene between 0.8 and 0.6 ka BP (ca.1100 - 1300 CE) and between 0.2 and 0.15 ka BP (ca.1750-1810 CE). Excluding Heinrich 2 stadial, wetter conditions occurred from 25 to 22 ka BP. Additionally, wetter conditions occurred from 14.5 to 8.5 ka BP (excluding the Younger Dryas) and since 4.5 ka BP to present.

Indeed, paleo-precipitation reconstruction (Figure 8) was in agreement with the reconstruction of Lake Challa's surface levels, encompassing high stands and low stands, based on a high-resolution seismic-reflection stratigraphy survey (Moernaut et al., 2010; Buckles et al., 2016).

Besides, there was agreement of periods with drier conditions during the Younger Dryas (13.1- 11.7 ka BP) and Heinrich 1 stadial (15 – 18 ka BP) for Lake Challa area (based on BIT), Greenland composite (NGRIP-GISP2-GRIP) based on atmospheric CH_4 record, Greenland (NGRIP) based on ice core $\delta^{18}O$ with respect to GICC05 timescale, and Hulu/Dongge cave based on stalagmite $\delta^{18}O$ (Verschuren et al., 2009). Additionally, there was agreement of a period with wetter conditions between the Younger Dryas and Heinrich 1 stadial between the four hydroclimate stations. Such findings suggest that precipitation patterns for Lake Challa area during a period of the last 25 ka was largely influenced by teleconnections of natural atmosphere-ocean modes of climate variability including IOD and ENSO and meridional shifts in the average position of ITCZ.

Moreover, a study conducted by Wolff et al. (2011) revealed that thin varves from Lake Challa highly correlated with El Niño events (positive Niño3.4 values) during a period of the previous 155 years while thick varves highly correlated with La Niña events (negative

Niño3.4 values). Indeed, La Niña events were associated with existence of strong winds that enhanced upwelling of nutrients and intensification of seasonal blooms of algae and, consequently, the formation of thicker varves. To the contrary, El Niño events were associated with existence of weak winds that led to the formation of thinner varves. Basing on analysis of varve structure, El Niño events with high rainfall over Lake Challa area occurred in years of 1997/98, 1982/83, 1941/42, 1914/15, 1905/06 and La Niña events with low rainfall occurred in 1988/89, 1971/72, 1955/56, 1950/51, 1924/25, 1917/18, and 1897/98.

CONCLUSIONS AND RECOMMENDATIONS

This paper sought to assess linkages between precipitation changes in semi-arid lowlands of Mwanga District and both human-induced climate change and natural modes of climate variability across different temporal scales. Since the findings revealed statistically significant decrease of annual rainfall at both Same and NyM Meteorological stations, it was concluded that the human-induced climate change had occurred in the study area between the 1970s and 2010s. Besides, the findings revealed, during the same time and stations, statistically significant correlations between amounts of rainfall (September – February) and ENSO's Niño 3.4 index and between amounts of OND rainfall and IOD's DMI. In this regard, it was concluded that precipitation changes during short rainy seasons (*Vulis*) in the lowlands were significantly influenced by cycles of climate variability (namely, ENSO and IOD).

Indeed, rainfall fluctuations during the last 25 ka were also influenced and shaped by meridional shifts in the average position of ITCZ and zonal Hadley/Walker Cell dynamics in the Indian Ocean due to changes in insolation forces. Furthermore, the findings revealed higher average coefficient of variation for rainfall at NyM Meteorological Station and lower average coefficient of variation for rainfall at Same Meteorological Station. In this respect, it was concluded that rainfall variability at Same Meteorological Station was lower as influenced by, among other things, topographical factors and continentality.

Since increasing rainfall perturbations pose significant risks on economic activities, including rain-fed agricultural production systems, that provide livelihoods to the majority of residents in the study area, there is a need to undertake studies aimed at enhancing synergies between traditional environmental knowledge systems (TEKS) and modern-day environmental knowledge systems (MEKS) as early warning systems. With regard to TEKS, studies could focus on traditional weather prediction through observation of changing appearance and positions of astronomical objects, such as a moon/stars (*Ngalakeri* in Pare language) and fruiting/ripening of fruits of wild plants, such as *Mikayo* (*Salvadora persica)* and *Baobab (Adansonia digitata).* Pertaining to MEKS, studies could focus on ways of enhancing reliability of modern weather forecasting and timely dissemination of weather advisories to stakeholders.

CONFLICT OF INTERESTS

The authors have not declared any conflict of interests.

REFERENCES

Bast JL (2010). Seven theories of climate change. Chicago, IL: Heartland Institute.

Brown DA (2013). Climate change: Navigating the perfect moral storm. London: Routledge.

Buckles LK, Verschuren D, Weijers JWH, Cocquyt C, Blaauw M, Sinninghe Damsté JS (2016). Interannual and (multi-) decadal variability in the sedimentary BIT index of Lake Challa, East Africa, over the past 2200 years: Assessment of the precipitation proxy. Climate of the Past 12:1243-1262.

Cassou C, Kushnir Y, Hawkins E, Pirani A, Kucharski F, Kang I–S, Caltabiano N (2018). Decadal climate variability and predictability: Challenges and opportunities. Bulletin of the American Meteorological Society 99(3):479-490.

FAO, IFAD, UNICEF, WFP, WHO (2018). The state of food security and nutrition in the world 2018. Building climate resilience for food security and nutrition. Rome, FAO. http://www.fao.org/3/I9553EN/i9553en.pdf

Field A (2013). Discovering statistics using IBM SPSS statistics. 4th Ed. London: SAGE.

Huang J, Ji M, Xie Y, Wang S, He Y, Ran J (2016). Global semi-arid climate change over last 60 years**.** Climate Dynamics 46(4):1131-1150.

Idso CD, Carter, RM, Singer SF (2016). Why scientists disagree about global warming: The NIPCC report on scientific consensus. 2nd Ed. Chicago, IL: Heartland Institute.

International Federation of Red Cross and Red Crescent Societies (IFRCRCS) (2013). Tanzania drought and food insecurity: Emergency appeal n° MDRTZ012 - final report. International Federation of Red Cross and Red Crescent Societies.

Inhofe J (2012). The greatest hoax: How the global warming conspiracy threatens your future. Washington, D. C: WND Books.

Intergovernmental Panel on Climate Change (IPCC) (2012). Managing the risks of extreme events and disasters to advance climate change adaptation. Cambridge: Cambridge University Press.

Intergovernmental Panel on Climate Change (IPCC) (2013). Climate change 2013: The physical science basis. Contribution of Working Group I to the Fifth Assessment Report of the IPCC. Cambridge: Cambridge University Press.

Kavishe FP, Mushi SS (1993). Nutrition-relevant actions in Tanzania. TFNC Monograph Series no. 1. UN ACC/SCN Country Study Supported by UNICEF. A Case Study for the XV Congress of the International Union of Nutritional Sciences, September 26 to October 1, 1993, Adelaide.

Kijazi AL, Reason CJC (2008). Analysis of the 1998 to 2005 drought over the northeastern highlands of Tanzania. Climate Research 38:209-223.

Laliberté F, Zika, J, Mudryk L, Kushner PJ, Kjellsson J, Döös K (2015). Constrained work output of the moist atmospheric heat engine in a warming climate. Science 347(6221):540-543.

Limbu F (1995). Agriculture and rural development in Tanzania: A survey of the 1980-1985 literature. Dar es Salaam: Economic and Social Research Foundation.

Mabhuye E, Yanda P, Maganga F, Liwenga E, Kateka A, Henku A, Malik N, Bavo C (2015). Tanzania: country situation assessment. PRISE working paper.

Mashingo M (2010). Vulnerability assessment on pastoral livestock and

pasture development to the extreme climatic events in Tanzania. Paper presented under the study on economics of climate change in Tanzania Phase 3, at the Stakeholder Inception Round Table Meeting held at the Peacock Hotel, Dar es Salaam, Tanzania, 26 March 2010.

Mwanga District Council (MDC) (2016). Mwanga district socio-economic profile. Mwanga: MDC. https://pefa.org/assessments/tanzania-mwanga-district-council-2016

Misana B, Sokoni C, Mbonile MJ (2012). Land-use/cover changes and their drivers on the slopes of Mount Kilimanjaro, Tanzania. Journal of Geography and Regional Planning 5(6):151-164.

Moernaut J, Verschuren D, Charlet F, Kristen I, Fagot M, De Batist M (2010). The seismic-stratigraphic record of lake-level fluctuations in Lake Challa: Hydrological stability and change in equatorial East Africa over the last 140 kyr. Earth and Planetary Science Letters 290:214-223.

Mvungi A (2008). The economy of affection/moral economy and water management for irrigation and environmental conservation in semi-arid areas: The case study of Mwanga district. In: Kimambo IN, Hyden G, Maghimbi S, Sugimura K (eds.). Contemporary perspectives on African moral economy. Dar es Salaam: Dar es Salaam University Press.

Ogwang BA, Ongoma V, Xing L, Ogou FK (2015). Influence of Mascarene high and Indian Ocean Dipole on East African extreme weather events. Geographica Pannonica 19 (2):64-72.

Ostberg S, Schewe J, Childers K, Frieler K (2018). Changes in crop yields and their variability at different levels of global warming. Earth System Dynamics 9:479-496.

Owiti Z, Ogallo LA, Mutemi J (2008). Linkages between the Indian Ocean Dipole and East African rainfall anomalies. Journal of Kenya Meteorological Society 2(1): 3-17.

Pokhrel S, Chaudhari HS, Saha SK., Dhakate A, Yadav RK, Salunke K, Mahapatra S (2012). ENSO, IOD and Indian Summer Monsoon in NCEP climate forecast system. Climate dynamics 39:2143-2165.

Røhr PC (2003). A hydrological study concerning the southern slopes of Mt Kilimanjaro, Tanzania. Dissertation (PhD), Norwegian University of Science and Technology.

Scroxton N, Burns SJ, McGee D, Hardt B, Godfrey LR, Ranivoharimanana L, Faina P (2017). Hemispherically in-phase precipitation variability over the last 1700 years in a Madagascar speleothem record. Quaternary Science Reviews 164:25-36.

Schmidt MW, Spero HJ (2011). Meridional shifts in the marine ITCZ and the tropical hydrologic cycle over the last three glacial cycles. Paleoceanography 26(1):PA1206.

Sinninghe Damsté JS, Ossebaar J, Schouten S, Verschuren D (2012). Distribution of tetraether lipids in the 25-ka sedimentary record of Lake Challa: Extracting reliable TEX86 and MBT/CBT palaeotemperatures from an equatorial African lake. Quaternary Science Reviews 50:43-54.

Stewart I (2008). Earth: The climate wars. London: BBC.

Tao T, Chaocat B, Liu S, Xin K (2009). Uncertainty analysis of interpolation methods in rainfall spatial distribution: A case of small catchment in Lyon. Journal of Environmental Protection 1:50-58.

United Nations (UN) (1992). United Nations framework convention on climate change. New York, NY: United Nations.

United Nations Environment Programme (2012). Global environment outlook GEO-5: Environment for development. Nairobi: UNEP.

United Republic of Tanzania (URT) (2004). Lake Jipe awareness raising strategy (2005–2007). Dar es Salaam: Ministry of Natural Resources and Tourism, Wildlife Division.

Verschuren D, Laird KR, Cumming BF (2000). Rainfall and drought in equatorial East Africa during the past 1100 years. Nature 403:410-414.

Verschuren D, Sinninghe Damsté JS, Moernaut J, Kristen I, Blaauw M, Fagot… Nowaczyk NR (2009). Half-precessional dynamics of monsoon rainfall near the East African Equator. Nature 462(7273):637-641.

Williams CA, Hanan NP (2011). ENSO and IOD teleconnections for African ecosystems: Evidence of destructive interference between climate oscillations. Biogeosciences 8:27-40.

Wolff C, Haug GH, Timmermann A, Sinninghe Damsté JS, Brauer A, Sigman DM, Cane MA, Verschuren D (2011). Reduced inter-annual rainfall variability in East Africa during the last ice age. Science 333:743-747.

Yeh S-W, Cai W, Min S-K, McPhaden MJ, Dommenget D, Dewitte B, Kug J-S (2018). ENSO atmospheric teleconnections and their response to greenhouse gas forcing. Reviews of Geophysics 56(1):185-206.

Zheng J, Yu Y, Zhang X, Hao Z (2018). Variation of extreme drought and flood in North China revealed by document-based seasonal precipitation reconstruction for the past 300 years. Climate of the Past 14:1135-1145.